EEG brain states for real-time detection of covert cognition in disorders of consciousness

Gabriel A. Della Bella,[1,2,†] Di Zang,[3,4,5,6,7,†] Peng Gui,[8,†] Diego M. Mateos,[9,10] Jacobo D. Sitt,[11,12] Tristan A. Bekinschtein,[13] Dragana Manasova,[11,14] Benjamine Sarton,[15,16] Fabrice Ferre,[15,16] Stein Silva,[15,16] Pedro W. Lamberti,[2,17] Xuehai Wu,[3,4,5,6,7] Ying Mao,[3,4,5,6,7] Liping Wang,[8*] and Pablo Barttfeld,[1*]

[†]**These authors contributed equally to this work.**

[*]**Co-senior authors.**

Abstract

One of the biggest challenges in cognitive neuroscience is developing diagnostic tools for Disorders of Consciousness (DoC). Detecting dynamical connectivity brain states seems promising, specifically those linked to transient moments of enhanced cognitive states in patients. A growing body of evidence indicates that fMRI brain states properties are strongly modulated by the level of consciousness , as theoretically predicted by whole brain modeling. fMRI-based brain states, however, have very limited practical application due to methodological constraints.

In this work we defined EEG-based brain states and explored their potential as a bedside, real-time tool to detect transient windows of enhanced brain states. We analysed data from 237 individual patients with chronic and acute DoCs -100 Unresponsive Wakefulness Syndrome (UWS), 96 Minimally Conscious State (MCS) and 41 acute- and 101 healthy controls obtained in three independent research centers (Fudan hospital in Shanghai, Pitié Salpêtrière in Paris and Purpan hospital in Toulouse).

We determined five EEG functional connectivity brain states, and show that their probability of occurrence is strongly related to the level of consciousness. Distinctively, high entropy brain states are exclusively found in healthy subjects, while low-entropy brain states increase their probability with DoC's severity, spanning from acute unarousable comatose state, to more chronic DoC's patients, who are awake but show fluctuating (MCS) or absent awareness (VS). Furthermore, the brain state probability distribution of each individual subject —and even the presence of certain key brain states— significantly vary with the patients' outcome. We also

tested whether our procedure has an actual potential for real-time, bedside brain state detection, and proved that we can reliably estimate the concurrent brain state of a patient in real time, paving the way for a broad application of this tool for DoC patients' diagnosis, follow-up, and neuroprognostication.

Author affiliations:

1 Cognitive Science Group. Instituto de Investigaciones Psicológicas (IIPsi,CONICET-UNC), Facultad de Psicología, Universidad Nacional de Córdoba, Córdoba, Argentina

2 Facultad de Matemática Astronomía y Física (FaMAF), Universidad Nacional de Córdoba. Córdoba, Argentina.

3 Department of Neurosurgery, Huashan Hospital, Shanghai Medical College, Fudan University,Shanghai, 200040, China

4 National Center for Neurological Disorders, Shanghai, 200040, China

5 Shanghai Key Laboratory of Brain Function and Restoration and Neural Regeneration, Shanghai, 200040,China

6 Neurosurgical Institute of Fudan University, Shanghai, China.

7 Shanghai Clinical Medical Center of Neurosurgery, Shanghai, China

8 Institute of Neuroscience, Key Laboratory of Primate Neurobiology, CAS Center for Excellence in Brain Science and Intelligence Technology, Chinese Academy of Sciences, Shanghai 200031, China

9 Facultad de Ciencia y Tecnología, Universidad Autónoma de Entre Ríos (UADER), Oro Verde E3100, Argentina

10 Instituto de Matemática Aplicada del Litoral (IMAL-CONICET-UNL). Santa Fe, Argentina

11 Sorbonne Université, Institut du Cerveau–Paris Brain Institute–ICM, Inserm, CNRS, APHP, Hôpital de la Pitié Salpêtrière, Paris, France.

12 Inserm U 1127, F-75013 Paris, France

13 Department of Psychology, University of Cambridge, Cambridge, CB2 3EB, United Kingdom

14 Université Paris Cité, Paris, France.

15 Réanimation URM CHU Purpan, Cedex 31300 Toulouse, France

16 Toulouse NeuroImaging Center INSERM1214, Cedex 31300 Toulouse, France

17 Institute of Theoretical Physics, Jagiellonian University, ul. Łojasiewicza 11, 30–348 Kraków, Poland

Correspondence to: Pablo Barttfeld

Blvd. de La Reforma esq. Enfermera Gordillo.

Ciudad Universitaria -5000- Córdoba. Argentina

pablob@conicet.gov.ar

Running title: EEG real-time detection of consciousness

Keywords: disorders of consciousness; electroencephalography; brain states; diagnosis; real-time.

Abbreviations: CRS-R = Coma Recovery Scale Revised; DoC = Disorders of Consciousness; GCS = Glasgow Coma Scale; LZC = Lempel Ziv Complexity; MCS = Minimally Conscious State; RT = real-time; UWS = Unresponsive Wakefulness Syndrome; wSMI = weighted Symbolic Mutual Information; WE = Weighted Entropy.

Introduction

Diagnosing disorders of consciousness (DoC) and prognosing the patients' evolution remain a major medical challenge. DoC classification is currently based on arousal and awareness clinical examination —to allow patient's labeling into a heterogeneous set of categories whose precise definitions are still evolving.[1,2] It has been argued that these clinical examinations are intrinsically hindered by its behavioral nature. Indeed, assessments of key cognitive processes underpinning consciousness recovery are subjective and limited to "overt" cognitive processes. Therefore, they are prone to biases due to confounding factors affecting patients' motor output

activity (e.g. locked-in syndrome)[3,4] or language processing (e.g. aphasia).[5,6] This results in a high diagnostic error rate, estimated at 40 percent,[7] that many times decides upon the patient's life.

Built upon the theoretical framework of connectionist theories of consciousness,[8–12] several neuroimaging tools have been recently proposed to inform the clinician of "covert" cognitive processes, obscure to bedside behavioral examinations. These techniques include measures relying on active cognitive tasks,[13–17] measures based on spontaneous brain activity,[18–22] and methods based on the combination of physical external stimulation and EEG responses.[8,23,24]

Among these methods, one of the most promising is based on studying signatures of consciousness through the detection of fMRI-based "brain states",[19,25–28] which is especially well suited to detect spontaneous, transient windows of covert cognition. Brain states are recurrent functional connectivity patterns obtained by unsupervised clustering of dynamical connectivity matrices usually lasting anywhere from 5 to 60 seconds.[25] Research shows that the properties of the brain states are strongly modulated by arousal levels and consciousness levels. In awake humans and monkeys there is a rich variety of brain states —including states of high connectivity, high entropy, and negative correlations.[19,25,26,28] By contrast, in DoC or under sedation the brain states found radically change: the richer brain states disappear and the repertoire of possible configurations becomes smaller —only low-connectivity, low-entropy states shaped by the underlying structural connectivity remain.[18,26] These findings are inline with dynamical systems simulations[29–31] showing that, for low coupling strength between brain areas —a configuration resembling DOC condition—spontaneous neuronal activity is still present but restricted to a single stable connectivity pattern, defined by the fixed network of structural connectivity. As connectivity between brain regions increases, the system transitions to multistability, with a diverse set of possible patterns. This transition is deemed paramount at sustaining conscious states.

However, currently brain states are defined for fMRI —an expensive technique ill-suited for DoC evaluation. DoC patients are difficult to transfer to the scanner, many times carrying life-supporting electronic (MRI incompatible) devices. Furthermore, detecting windows of momentarily enhanced covert cognition involves repeated assessments across long periods, which is impossible to perform in an MRI scanner. In contrast, EEG-defined brain states estimated bedside could become an invaluable tool as they allow for real-time brain state detection. This would open the possibility for a more accurate evaluation of residual brain

activity in DoC patients to eventually allow designing optimal individually-tailored medical-patient interaction and stimulation in their windows of responsivity.

For this research, we studied one of the largest reported DoC patient cohorts —237 patients and 101 controls from three independent research sites— to bring EEG-based consciousness detection closer to a reality in clinical settings. Contrary to previous reports which have been based almost exclusively on chronic DoC data —Unresponsive Wakefulness State (UWS) and Minimally Conscious State (MCS)—, we combined data from chronic patients and acute patients (i.e. comatose) to define EEG brain states and study its potential as a diagnostic and prognostic tool along the entire DoC axis (Fig. 1A). We found and characterized EEG functional connectivity brain states, and showed that their probability of occurrence is strongly related to the level of consciousness. In particular, high entropy brain states are almost exclusively found in conscious subjects, while low-entropy brain states increase their probability with DoC severity. We found that patients displayed transient patterns of functional connectivity that resembled high entropy brain states characteristic of healthy subjects. These patterns' probability of occurrence was informative regarding DoC diagnosis and even the outcome of each patient. We finally showed that these transient states of enhanced connectivity —possibly reflecting transient moments of enhanced covert consciousness— could be reliably detected in a bedside, real-time setting (Fig. 1B).

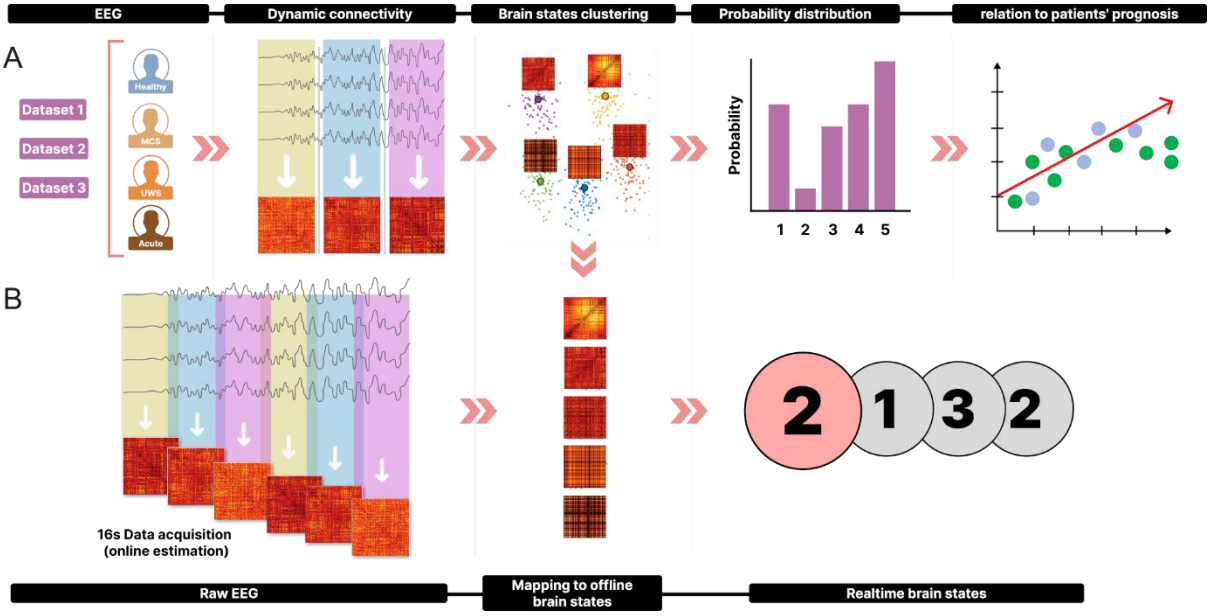

Figure 1. Analysis pipeline. A) Offline calculation of brain states. Three datasets were used from three different Centers, including healthy controls and three patients categories (minimally conscious state [MCS], uws Unresponsive Wakefulness State [UWS] and Acute patients). After obtaining windowed wSMI matrices we performed a clustering analysis to obtain 5 brain states, whose probability and relation to patient's prognosis was estimated. B) Real-time calculation of brain states. Simulating a bedside situation, we processed every 20 s, 16 s of raw EEG data to obtain raw-data wSMI matrices. Using previously obtained brain states, we mapped wSMI matrices into the closest brain state, obtaining this way a real time brain state.

Materials and methods

Ethics statement

All data collections have been approved by their respective ethical committees. The Shanghai study was approved by the Ethical Committee of the Huashan Hospital of Fudan University (approval number: HIRB-2014-281). The Paris study was approved by the Ethical Committee of the Pitié Salpêtrière under the French label of '*Recherche en soins courants*' [routine care research]. The Toulouse study was approved by the ethics committee of the University Hospital of Toulouse, Toulouse, France (approval number: RC 31/20/0441). All data collections and analyses were carried out in accordance with the Declaration of Helsinki.

Participants and Recordings

A total of 237 patients and 101 control subjects were included in the present study (Table 1). The EEG recording systems used by the three data collections were Electrical Geodesics (HCGSN, 257-channel net cap for the Shanghai and Paris datasets, 128-channels for the Toulouse dataset) sampled at 1000 Hz for Shanghai and 250 Hz for Paris and Toulouse. For computational purposes and to match the electrode number between datasets we downsampled the Shanghai and Paris datasets to 128 channels, using the locations of the Hydrocel Geodesic Sensor Net-128, by applying the default interpolation method provided by EEGLAB.[32] Some participants contributed more than one EEG recording (in these cases we averaged within subjects results prior to statistical analysis). Age and gender distributions were similar across datasets (Table 1). The Toulouse dataset was composed of task-free EEG recordings of acute patients, and the Shanghai and Paris datasets were composed of task-related EEG data from chronic (MCS and UWS) patients. Multiple clinical assessments were performed by trained clinicians, including CRS-R scoring.[33,34] See supplementary methods for tasks and diagnostic details.

Dynamic wSMI calculation

The wSMI is a measure of shared information that detects nonrandom joint fluctuations between two EEG signals (i.e: two channels). All details of the procedure can be found in King et al.[15] The first step is transforming the signals into a string of symbols. We set the parameters length of the symbol d to 3, and their temporal separation τ to 8 ms. After translating the two signals from different electrodes into symbols, the joint probability is computed. A modified version of the canonical mutual information is used, dismissing the interaction between similar symbols to remove spurious correlations between EEG signals arising from common sources.[15,17]

To make wSMI dynamic, for every EEG session we considered a series of rectangular windows of length 16 seconds shifted by 1 second. Within each window, we computed wSMI, producing 128x128 symmetric connectivity matrices per window and subject. The number of windows was different for each subject as it depends on the session length. The Shanghai dataset has 465 windows per subject while the Paris dataset has 1300 ± 300 (mean ± SD) windows and the Toulouse dataset has 1800 ± 800 windows per subject.

Unsupervised clustering of connectivity matrices

We applied the k-means clustering algorithm to obtain recurring patterns of connectivity, as previously performed in fMRI[19,25] and EEG[35,36] .We down-sampled the number of windows of each subject to 300 (using a larger number of windows per subject did not change the results). The purpose of this downsampling is twofold: subsampling reduces the required computational resources, and more importantly, makes each EEG recording equally represented in the clustering algorithm. We set the number of clusters to k = 5, the number of replicates to 10,000, and we used the Manhattan distance as a measure for distance, as done in the literature.[25] The number of clusters k was chosen using the elbow method where the explained variation is plotted against a wide range of k values (3 through 6 in our case) and the optimal k is the one where the graph begins to plateau. Replicating prior research, our results are not critically dependent on the number of clusters (Fig. S1). After obtaining the centroids, we classified each individual connectivity matrix into one of the five centroids or brain states according to their distance to the closest brain state.

Brain state complexity and distribution across DoC

The brain states obtained by k-means clustering were ordered by decreasing entropy. This was done by calculating the entropy of the distribution of wSMI values for each centroid. We also calculated the Lempel-Ziv complexity (LZC) for each centroid, which is a measure of the irreducible information contained in a sequence. The probability of occurrence of each brain state was estimated as the proportion of times each individual connectivity matrix was classified as belonging to that brain state.

To quantify how brain state distributions shifted towards certain brain states we defined a weighted entropy (WE) , as:

$$WE = \sum_{i=1}^{5} p_i \cdot (1 - H_i) \qquad (1)$$

Where p_i is the probability of each brain state and H_i is its entropy.

Patients' Outcome

We assessed the evolution of patients to explore how brain states might be informative of their prognosis. For chronic patients, we defined the possible outcomes as improvement of the clinical condition (UWS patients becoming MCS, MCS patients becoming MCS+), deterioration (patients dying or going from MCS to UWS), or unchanged clinical condition. Similarly, for acute patients we defined the outcomes based on how they evolved from acute condition: clinical condition evolving to MCS, to UWS or dying.

Real-time simulation

We conducted, as a proof of concept, a real-time simulation analysis where we processed, every 22 seconds, 16 seconds of raw EEG signal from acute patients, simulating real-time data collection and processing. We filtered each segment between 1 and 40 Hz, and no other preprocessing or cleaning step was conducted (crucially, no window was discarded). For each 16 seconds EEG signal we estimated a 128 x 128 wSMI matrix and calculated the distance between this "real-time" matrix and the brain states previously defined offline. To explore results variability due to brain states definition, we used three different offline brain states estimations to classify the real-time matrices: 1) brain states defined for all participants, b) brain states defined for patients only and c) brain states defined for the acute patients and their controls. We then estimated how real-time and offline brain state classification compared.

Statistics

To quantify group differences, we conducted mixed linear models in R[37] using RStudio 1.3.1073 with packages *lme4*, with the equation WE ~ Group + (1|Center) where WE is the weighted entropy of each participant, Center is a categorical variable indexing the Shanghai, Paris and Toulouse datasets respectively, and Group is also a categorical variable for Healthy, MCS, UWS and Acute. To get p-values for the group effect WE values were submitted to a linear mixed model using the mixed function from the *afex* package, using the Kenward-Roger approximation. We also conducted post-hoc comparisons between Healthy, MCS, UWS and Acute using the function lsmeans (package *lsmeans*).

To quantify the effect of rate on the chronic patient's outcome we conducted a mixed linear models with the equation WE ~ Outcome + (1|Center). For the effect of WE on the acute patient's outcome we did not conduct a mixed linear model since acute patients' data is only represented in the Toulouse dataset (i.e. no random variable 'Center'); we conducted an ANOVA with the equation WE ~ Outcome using the *aov* function in R.

To quantify the distance between real-time and offline estimations of brain states we followed a bootstrap and Jensen Jannon distance analysis.

Let P = $\{p_1, \ldots, p_n\}$ and Q = $\{q_1, \ldots, q_n\}$ be two probability distributions, the Jensen-Shannon distance is defined as:

$$JS(P,Q) = \sqrt{\frac{1}{2}(KL(P \mid\mid \frac{P+Q}{2}) + KL(Q \mid\mid \frac{P+Q}{2}))} \qquad (2)$$

where KL(P || Q) is the Kullback-Leibler divergence defined as:

$$KL(P \mid\mid Q) = \sum_{i=1}^{n} p_i \cdot ln(\frac{p_i}{q_i}) \qquad (3)$$

We divided the set of acute patients into two random groups of 20 subjects and calculated the average probability distribution of each set, as classified by the offline acute brain states. Then, we computed the Jensen-Shannon distance between them and repeated this procedure 10,000 times to generate a distribution of distances. We divided again into two random groups of 20 but the second group was classified using the real-time brain states. By comparing these two distributions we can estimate how different real-time and offline classifications are.

Software

All data was processed using custom MatLab, R and Python software, using specific libraries. We used the Python libraries Nice,[38] MNE[39] and scikit-learn.[40] Codes are available at https://github.com/dellabellagabriel/doc-brain-states

Results

Detection of EEG brain states

We first explored whether brain states can be meaningfully found in EEG. We found five EEG-brain states, showing distinctive connectivity patterns (Fig. 2A). These patterns are robust, as we detected them when varying the number of brain states from 3 to 10 (Fig. S1) and when exploring all datasets separately (Fig. S2). We sorted the brain states according to their entropy level (Fig. 2A) and we numbered them in decreasing order. Consistently with previous findings in fMRI,[19,26–28] brain states 1 and 2 —showing the highest entropy and complexity (Fig. 2B)— displayed the largest connectivity range, including both weak and strong connections between electrodes in a well-defined topographical map. They show two clear, bilateral parietal hubs of connectivity including long distance connectivity (Fig. S3). Brain state 1 was characterized by the highest complexity and entropy (Fig. 2B), reflecting a conserved brain wide functional network coordination typically associated with the awake state.[19] In the other extreme of the entropy scale, brain states 4 and 5 had a markedly different pattern: a very narrow, low connectivity range in which connections are homogeneously distributed in the scalp (Fig. 2A) across all electrode distances (Fig. S3). A hierarchical decomposition analysis of the brain state space revealed the similarities —and their positions in the multidimensional space— between brain states. A cluster composed by states 4 and 5 were the most similar ones, subsequently merging with brain states 3 and 2 (Fig. 2D). Brain state 1 merged the remaining ones at a very high distance (Fig. 2D).

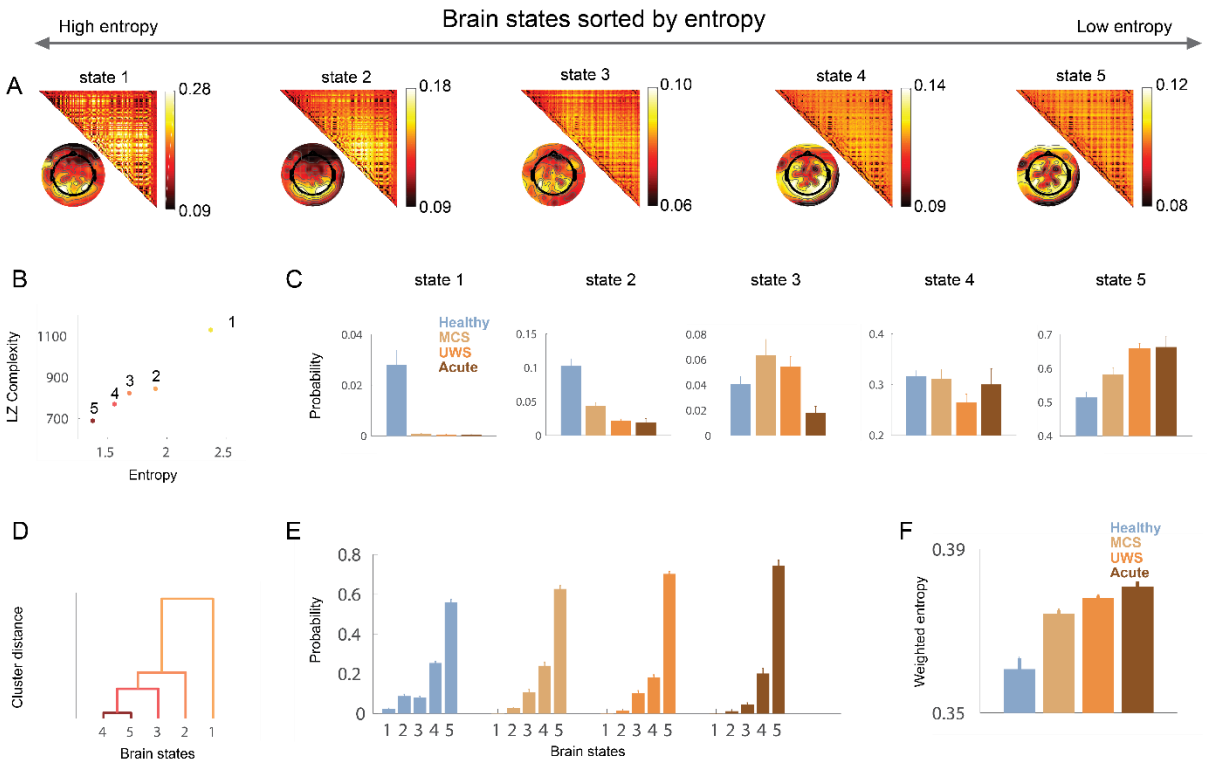

Figure 2. EEG brain states and their distribution DOC. A) brain states ordered by entropy from 1 (high entropy) to 5 (low entropy). Topoplot colormaps limits are set to their max and min values. Brain states 1, 2, and 3 have a wide variety of values whereas states 4 and 5 have more uniform wSMI values. B) Lempel-Ziv complexity as a function of entropy for every brain state. States with a greater variance will have higher values of entropy and LZ complexity as well. C) Brain states probability distributions across all groups. Brain state 1 is mostly present in healthy subjects, whereas brain state 5 increases its probability with DoC severity. D) Dendrogram clustering showing distances between brain states. E) Brain states probability distributions for all groups. Mass distribution shifts towards high values as DoC severity increases. F) Weighted entropy for all groups.

EEG brain states rates of occurrence across levels of consciousness

DoC modulated brain state distribution across groups (Fig. 2C, D). Weighted entropy (WE) shifted towards higher values in patients as compared to controls as DoC severity increased from MCS to UWS to acute (Fig. 1E) ($F_{(3,153.1)}$ = 25.45, p = $2x10^{-13}$). Using the centroids obtained from both controls and patients data we found signitivative differences between controls and all patient's groups (Healthy vs. MCS [t-ratio$_{(294.8)}$ = -4.497, p = 0.0001], Healthy vs. UWS [t-ratio$_{(294.9)}$ = -6.081, p < 0.0001], Healthy vs. Acute [t-ratio$_{(82.1)}$ = -5.967, p < 0.0001]) but, within patients, only between MCS and Acute ([t-ratio$_{(54.1)}$ = -2.883, p = 0.028]). Both the probability of each state (Fig. 2C) and the average weighted entropy (Fig 2F) were

consistently modulated by the participant's condition: As the level of consciousness decreases, the probability of high entropy diminishes (Fig. 2C, left panels), the probability of low-entropy states increases (Fig. 2C, right panels) and the average weighted entropy increases (Fig. 2F).

EEG brain states and their relation with patients' diagnosis and prognosis

Next, we run the clustering algorithm excluding control subjects' data, to zoom in the region of the multidimensional space the patients data occupy, and obtain a finer-grained clustering. The new brain states greatly resembled those including control subjects data (Fig. 3A and Fig. S1). New brain state 1 displays a similar topography than brain state 1 in Fig. 2A, although with lower entropy values (consistent with the fact it is calculated on patients data only), suggesting that some patients display traces of awake-like brain states. As expected from our earlier analysis, both the probability of each individual state (Fig 3B) and WE (Fig 3C, D) changes across groups. To quantify this, we performed another mixed linear model analysis. Weighted entropy (WE) shifted towards higher values in patients as compared to controls as DoC severity increased from MCS to UWS to acute (Fig. XE) ($F_{(3,183.82)} = 18.7$, $p = 1.2x10^{-10}$). Using the centroids obtained from patients' data only we found signitivative differences between patient's groups (MCS vs. UWS [t-ratio$_{(332.1)}$ = -2.793, $p = 0.0282$]; MCS vs. Acute [t-ratio$_{(72.2)}$ = -3.879, $p = 0.0013$]; UWS vs. Acute [t-ratio$_{(71.6)}$ = -2.641, $p = 0.0487$], Fig. 3D).

Next we explored the potential of our methodology in patient's prognosis. We found a significant relation between patients' outcome and WE both for chronic ($F_{(2,178.6)} = 5.03$, $p = 0.007$; Fig. 3E) and Acute ($F_{(2,38)} = 5.947$, $p = 0.00566$; Fig. 3F) patients. Patients improving their condition showed a lower WE entropy. In contrast, those patients that were going to worsen their medical condition had higher weighted average entropy.

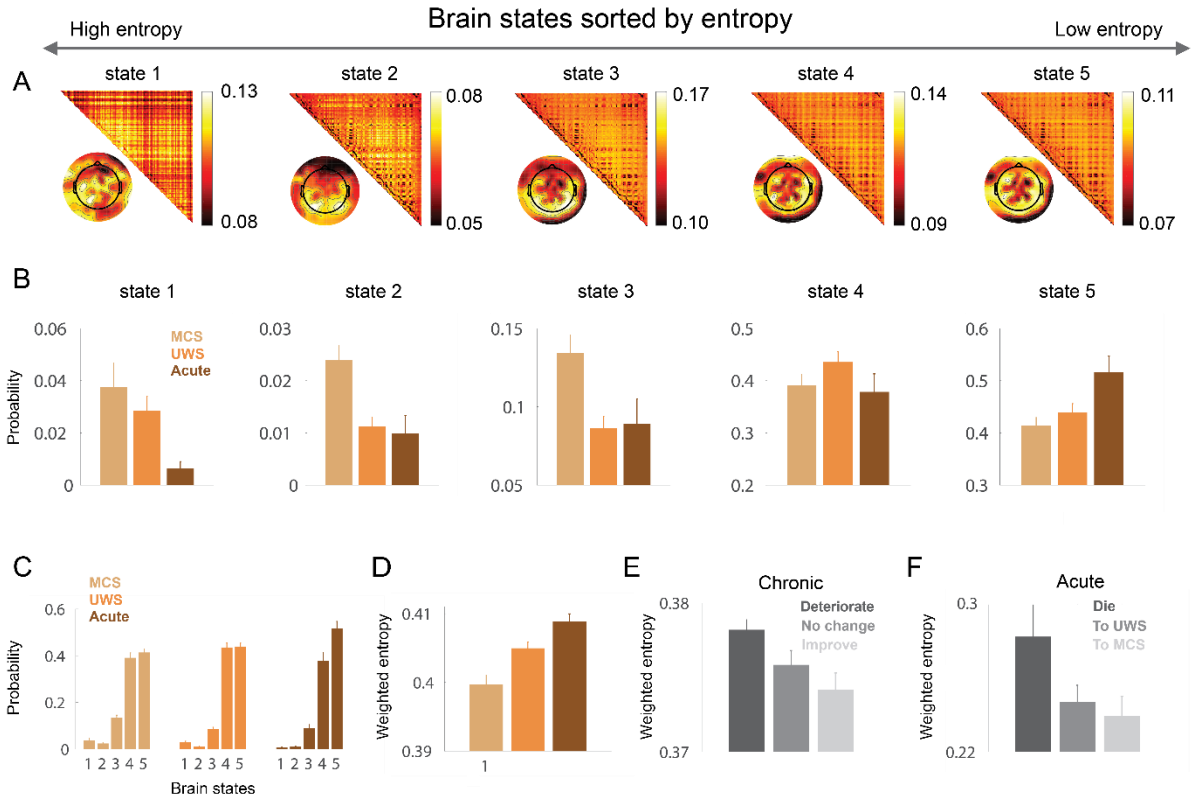

Figure 3. Brain states in diagnosis and prognosis. A) brain states defined including only patients data. Topoplot colormaps limits are set to their max and min values. B) Probability distribution of all 5 brain states across all groups. New brain states 1 and 2 now appear in all groups and monotonically diminishes with DOC severity, while brain state 5 increases its probability with DoC severity. C) Brain states probability distributions for all groups. D) Weighted entropy for all groups. E) Weighted entropy as a function of chronic patients' outcome. E) Weighted entropy as a function of acute patients' outcome.

Real-time simulation

Lastly, we explored the actual potential of our methodology in real-time, bedside settings. We calculated windowed wSMI for each segment of raw EEG signal and mapped them into one of the five previously defined brain states from the same patients (Fig. 1B, 4A). For comparison purposes we also classified the matrices against brain states calculated for all patients (Fig. 4B) and all participants (Fig. 4C). Then we estimated how different online and offline brain states distributions are, using the Jensen Jannon divergence. The divergence between RTs and offline distributions was not significantly different from random fluctuations when classifying real-time data according to the offline brain states of the same patients (Fig. 4A, $p = 0.81$) and all patients (Fig. 4B, $p = 0.28$). However, the distance between real-time and offline was significantly different from random fluctuations when considering all participants (Fig. 4C, $p =$

0.0007), evidencing that brain state definition strongly affected the real-time brain state definition.

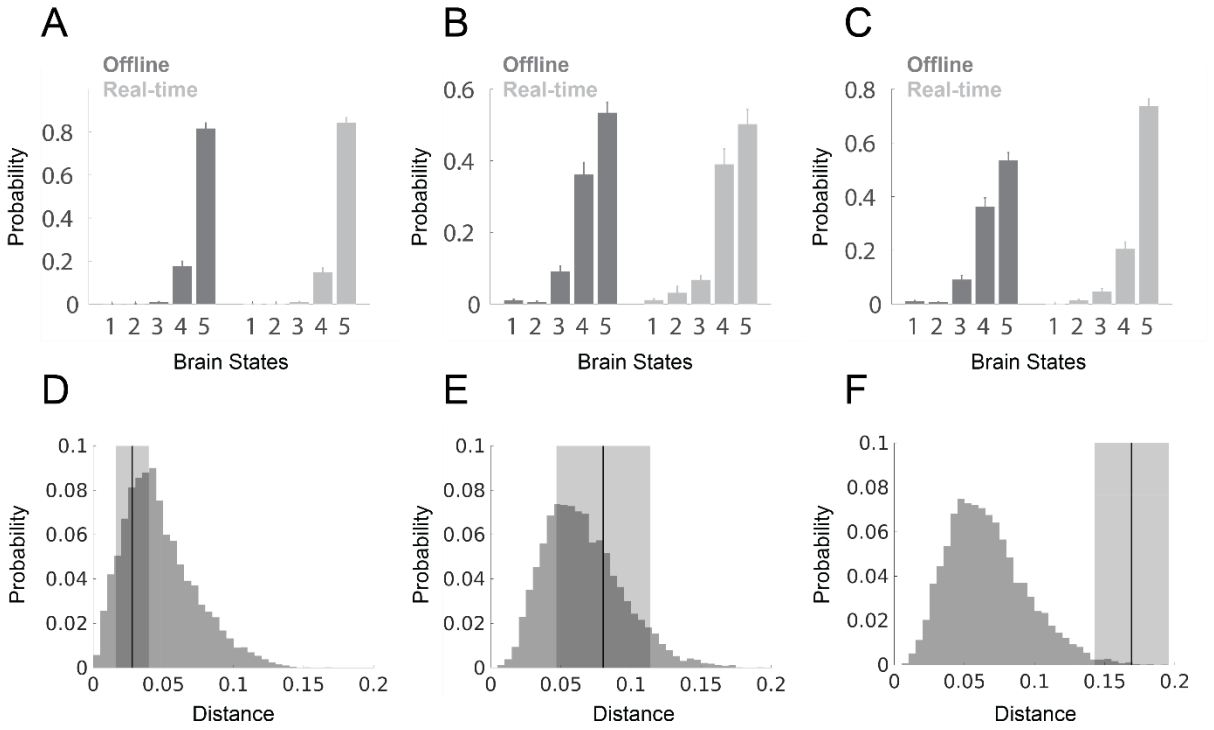

Figure 4. Estimation of EEG brain states in a real-time simulation. Offline and real-time probability distributions for brain states of acute patients estimated using offline centroids of acute patients only (A and D), all patients (B and E) and all participants (C and F).

Discussion

In this work we defined EEG brain states and studied their characteristics in healthy subjects and DoC patients. We identified recurrent brain states and showed that their rate of occurrence indexed the patient's category and recovery probability. We also successfully tested whether our procedure has an actual potential for real-time, patient's bedside brain state detection, and showed that indeed we can reliably estimate in real time the brain state a patient is in.

Brain states and DoC connectivity

Our results are in line with previous findings on DoC functional connectivity, as EEG brain states presented topographical patterns consistent with already published connectivity patterns in wakefulness and DoC.[19,25,26] Brain states 1 and 2 showed a remarkable similarity with topographies found in healthy subjects in time-averaged wSMI estimations[15,17] and correlations in fMRI.[19] This topography reflects a temporal organization involving long-range coupling

between brain regions that creates discrete functional connectivity patterns[19] characterized by the presence of both positive and negative correlations and a clear connectivity hub at bilateral parietal cortices. Brain states 4 and 5 also displayed recognizable patterns, being similar to patterns found using fMRI in anesthetized monkeys[26–28] and DoC patients[15,19] in EEG and fMRI: highly distributed, homogeneous low connectivity, without negative correlations.

Theory and modeling

Our results are also consistent with theories of consciousness based on experimental and modeling work which emphasize the role of long-distance connectivity underlying conscious emergence and mantainence.[10,30] Current whole brain models of consciousness propose that rich functional dynamics constitutes a signature of consciousness, and these dynamics can only be sustained at a certain minimal value of coupling between brain regions. At high coupling values there is a continuous and transient exploration of the global workspace, allowing the brain to combine segregated and integrated neural dynamics supporting consciousness.[8,23,41] When brain regions start to decouple —due to anesthesia, injury as in DoC, or NREM sleep[29,30]— functional connectivity converges into a pattern of low connectivity resembling the anatomy, very stable and long-lasting. This brain state is neither segregated or integrated, as is spatially homogeneously and weakly connected.

Using EEG instead of fMRI implies a big methodological challenge for studying brain states and its modeling. fMRI signals can be traced to a given brain region and, therefore, a relation between functional and structural connectivity can be established. Research shows that structural matrices constrain functional connectivity and shape brain states under low states of vigilance. The brain activity resided most frequently in a pattern of low connectivity resembling the anatomy, which was sustained for longer periods of time in comparison to more complex patterns.[26,28] The similarity-to-structure organizes the dimension along brain states, from those exclusive of conscious condition to those dominating under low vigilance. In this work we experimentally overcame the lack of a structural connectivity backbone by organizing brain states according to their entropy level.

Our results indicate that this sorting highly resembles the anatomical sorting of brain states. This similarity suggests that a precise mapping between EEG and fMRI brain states could be possible. Future work should study how to model and fit our results without using a structural matrix, starting an EEG brain states-based modeling possibly relying on a functionally defined connectivity backbone instead of an anatomical one.

Patients' classification and outcome.

Using EEG brain states we were able to discriminate between controls and patients, and, more importantly, between DoC categories. Our aim was not to achieve outstanding brain state-based classification scores, since using a single methodological approach could hardly outperform recently proposed methods based on combining multiple metrics in a multimodal approach.[38,42,43] The combination of current EEG classification methods with the detection of transient windows of covert cognition might provide an invaluable tool for patients' diagnosis and prognosis[44]. Furthermore, even complex brain states presence was indicative of DoC category and patients' outcome. Given that the DoC nomenclatures themselves are still under examination and their boundaries and number of categories are not entirely clear, DoC definitions might be updated to consider the presence of complex brain states supporting transient moments of covert consciousness.

Practical implications and bedside assessment

EEG brain states allow for the possibility of bedside, real-time states detection and the identification of windows of enhanced responsiveness for subsequent intervention. As mentioned, richer brain states practically disappear in patients, but traces of them are identifiable in all DoC categories. This suggests that the patients' brain briefly visits configurations close to the richest brain states —although with much lower average connectivity. This transiently rich brain state seems a good candidate to identify windows of momentarily enhanced cognition in patients, whose detection could serve for optimal communication and intervention. An intervention during brief states of covert consciousness might produce a sustained exploration of the brain state repertoire and their associated behavioral changes. fMRI brain states in anesthetized monkeys have proven to capture changes due to deep-brain stimulation, and a similar approach might be useful in DoC patients, driving

the brain state towards cognitively rich configurations. This is especially appealing since our results remain virtually unchanged when using a low-density electrode set-up (Fig. S4).

Conclusions

In this study, we showed that EEG brain states distribution and properties are strongly related to the level of consciousness. High-entropy brain states are almost exclusively found in conscious subjects, while low-entropy brain states increase their probability with DoC severity. We also found that these patterns' probability of occurrence was informative of the patient's prognosis. We finally demonstrated that these transient states of enhanced connectivity — possibly reflecting transient moments of enhanced covert consciousness— could be reliably detected in a bedside, real-time setting.

Acknowledgements

We thank Rodrigo Echeveste, Srivas Chennu, Damian Cruse, Demian Engemann, Federico Raimondo and Anat Arzi for useful discussions

Funding

This research was supported by Agencia Nacional de Promoción Científica y Tecnológica, Argentina (Grants #2018-03614 and CAT-I-00083). LW was supported by the Lingang Laboratory, Grant No. LG202105-02-01 and the Shanghai Municipal Science and Technology Major Project 2021SHZDZX. PG was supported by the Youth Innovation Promotion Association Chinese Academy of Sciences. GDB and PB were supported by the National Scientific and Technical Research Council (CONICET - Argentina). DZ, YM and XW were funded by the Shanghai Municipal Science and Technology Major Project [2018SHZDZX01], ZJLab, by the Shanghai Center for Brain Science and Brain-Inspired Technology, and by the Lingang Laboratory, [grant number LG202105-02-03].

Competing interests

The authors report no competing interests.

Data availability

The clinical data used in this paper can be made available upon reasonable request, but because of the sensitive nature of the clinical information concerning the patients the ethics protocol does not allow open data sharing.

Supplementary material

Supplementary material is available at *Brain* online.

References

1. Edlow BL, Claassen J, Schiff ND, Greer DM. Recovery from disorders of consciousness: mechanisms, prognosis and emerging therapies. *Nat Rev Neurol*. 2021;17(3):135-156. doi:10.1038/s41582-020-00428-x
2. Naccache L. Minimally conscious state or cortically mediated state? *Brain*. 2018;141(4):949-960. doi:10.1093/brain/awx324
3. Formisano R, D'Ippolito M, Catani S. Functional locked-in syndrome as recovery phase of vegetative state. *Brain Inj*. 2013;27(11):1332-1332. doi:10.3109/02699052.2013.809555
4. Laureys S, Owen AM, Schiff ND. Brain function in coma, vegetative state, and related disorders. *Lancet Neurol*. 2004;3(9):537-546. doi:10.1016/S1474-4422(04)00852-X
5. Majerus S, Bruno MA, Schnakers C, Giacino JT, Laureys S. The problem of aphasia in the assessment of consciousness in brain-damaged patients. In: Laureys S, Schiff ND, Owen AM, eds. *Progress in Brain Research*. Vol 177. Coma Science: Clinical and Ethical Implications. Elsevier; 2009:49-61. doi:10.1016/S0079-6123(09)17705-1
6. Pincherle A, Rossi F, Jöhr J, et al. Early discrimination of cognitive motor dissociation from disorders of consciousness: pitfalls and clues. *J Neurol*. 2021;268(1):178-188. doi:10.1007/s00415-020-10125-w
7. Schnakers C, Vanhaudenhuyse A, Giacino J, et al. Diagnostic accuracy of the vegetative and minimally conscious state: Clinical consensus versus standardized neurobehavioral assessment. *BMC Neurol*. 2009;9(1):35. doi:10.1186/1471-2377-9-35
8. Casali AG, Gosseries O, Rosanova M, et al. A Theoretically Based Index of Consciousness Independent of Sensory Processing and Behavior. *Sci Transl Med*. 2013;5(198). doi:10.1126/scitranslmed.3006294
9. Dehaene S, Lau H, Kouider S. What is consciousness, and could machines have it? Published online 2017:8.
10. Dehaene S, Changeux JP. Experimental and theoretical approaches to conscious processing. *Neuron*. 2011;70(2):200-227. doi:10.1016/j.neuron.2011.03.018
11. Mashour GA, Roelfsema P, Changeux JP, Dehaene S. Conscious Processing and the Global Neuronal Workspace Hypothesis. *Neuron*. 2020;105(5):776-798. doi:10.1016/j.neuron.2020.01.026
12. Tononi G, Boly M, Massimini M, Koch C. Integrated information theory: from

consciousness to its physical substrate. *Nat Rev Neurosci*. 2016;17(7):450-461. doi:10.1038/nrn.2016.44
13. Bekinschtein TA, Dehaene S, Rohaut B, Tadel F, Cohen L, Naccache L. Neural signature of the conscious processing of auditory regularities. *Proc Natl Acad Sci*. 2009;106(5):1672-1677. doi:10.1073/pnas.0809667106
14. Faugeras F, Rohaut B, Weiss N, et al. Probing consciousness with event-related potentials in the vegetative state. *Neurology*. 2011;77(3):264-268. doi:10.1212/WNL.0b013e3182217ee8
15. King JR, Sitt JD, Faugeras F, et al. Information Sharing in the Brain Indexes Consciousness in Noncommunicative Patients. *Curr Biol*. 2013;23(19):1914-1919. doi:10.1016/j.cub.2013.07.075
16. Owen AM, Coleman MR, Boly M, Davis MH, Laureys S, Pickard JD. Detecting Awareness in the Vegetative State. *Science*. 2006;313(5792):1402-1402. doi:10.1126/science.1130197
17. Sitt JD, King JR, El Karoui I, et al. Large scale screening of neural signatures of consciousness in patients in a vegetative or minimally conscious state. *Brain*. 2014;137(8):2258-2270. doi:10.1093/brain/awu141
18. Demertzi A, Antonopoulos G, Heine L, et al. Intrinsic functional connectivity differentiates minimally conscious from unresponsive patients. *Brain*. 2015;138(9):2619-2631. doi:10.1093/brain/awv169
19. Demertzi A, Tagliazucchi E, Dehaene S, et al. Human consciousness is supported by dynamic complex patterns of brain signal coordination. *Sci Adv*. 2019;5(2):eaat7603. doi:10.1126/sciadv.aat7603
20. Malagurski B, Péran P, Sarton B, et al. Topological disintegration of resting state functional connectomes in coma. *NeuroImage*. 2019;195:354-361. doi:10.1016/j.neuroimage.2019.03.012
21. Silva S, de Pasquale F, Vuillaume C, et al. Disruption of posteromedial large-scale neural communication predicts recovery from coma. *Neurology*. 2015;85(23):2036-2044. doi:10.1212/WNL.0000000000002196
22. Stender J, Gosseries O, Bruno MA, et al. Diagnostic precision of PET imaging and functional MRI in disorders of consciousness: a clinical validation study. *Lancet Lond Engl*. 2014;384(9942):514-522. doi:10.1016/S0140-6736(14)60042-8
23. Ferrarelli F, Massimini M, Sarasso S, et al. Breakdown in cortical effective connectivity during midazolam-induced loss of consciousness. *Proc Natl Acad Sci*. 2010;107(6):2681-2686. doi:10.1073/pnas.0913008107
24. Rosanova M, Gosseries O, Casarotto S, et al. Recovery of cortical effective connectivity and recovery of consciousness in vegetative patients. *Brain J Neurol*. 2012;135(Pt 4):1308-1320. doi:10.1093/brain/awr340
25. Allen EA, Damaraju E, Plis SM, Erhardt EB, Eichele T, Calhoun VD. Tracking Whole-Brain Connectivity Dynamics in the Resting State. *Cereb Cortex N Y NY*. 2014;24(3):663-676. doi:10.1093/cercor/bhs352
26. Barttfeld P, Uhrig L, Sitt JD, Sigman M, Jarraya B, Dehaene S. Signature of consciousness in the dynamics of resting-state brain activity. *Proc Natl Acad Sci*. 2015;112(3):887-892. doi:10.1073/pnas.1418031112
27. Tasserie J. Deep brain stimulation of the thalamus restores signatures of consciousness in a nonhuman primate model. *Sci Adv*. Published online 2022:18.
28. Uhrig L, Sitt JD, Jacob A, et al. Resting-state Dynamics as a Cortical Signature of Anesthesia in Monkeys. *Anesthesiology*. 2018;129(5):942-958. doi:10.1097/ALN.0000000000002336
29. Deco G, Cruzat J, Cabral J, et al. Awakening: Predicting external stimulation to force

transitions between different brain states. *Proc Natl Acad Sci*. 2019;116(36):18088-18097. doi:10.1073/pnas.1905534116
30. Kringelbach ML, Deco G. Brain States and Transitions: Insights from Computational Neuroscience. *Cell Rep*. 2020;32(10):108128. doi:10.1016/j.celrep.2020.108128
31. Sanz Perl Y, Pallavicini C, Pérez Ipiña I, et al. Perturbations in dynamical models of whole-brain activity dissociate between the level and stability of consciousness. Taylor PN, ed. *PLOS Comput Biol*. 2021;17(7):e1009139. doi:10.1371/journal.pcbi.1009139
32. Delorme A, Makeig S. EEGLAB: an open source toolbox for analysis of single-trial EEG dynamics including independent component analysis. *J Neurosci Methods*. 2004;134(1):9-21. doi:10.1016/j.jneumeth.2003.10.009
33. Giacino JT, Kalmar K, Whyte J. The JFK Coma Recovery Scale-Revised: measurement characteristics and diagnostic utility. *Arch Phys Med Rehabil*. 2004;85(12):2020-2029. doi:10.1016/j.apmr.2004.02.033
34. Wannez S, Heine L, Thonnard M, Gosseries O, Laureys S, Coma Science Group collaborators. The repetition of behavioral assessments in diagnosis of disorders of consciousness. *Ann Neurol*. 2017;81(6):883-889. doi:10.1002/ana.24962
35. Núñez P, Poza J, Gómez C, et al. Abnormal meta-state activation of dynamic brain networks across the Alzheimer spectrum. *NeuroImage*. 2021;232:117898. doi:10.1016/j.neuroimage.2021.117898
36. Núñez P, Gómez C, Rodríguez-González V, et al. Schizophrenia induces abnormal frequency-dependent patterns of dynamic brain network reconfiguration during an auditory oddball task. *J Neural Eng*. 2022;19(1):016033. doi:10.1088/1741-2552/ac514e
37. Team RC. R: A language and environment for statistical computing. R Foundation for Statistical Computing, Vienna, Austria. *HttpwwwR-Proj*. Published online 2016. Accessed July 15, 2022. https://cir.nii.ac.jp/crid/1574231874043578752
38. Engemann DA, Raimondo F, King JR, et al. Robust EEG-based cross-site and cross-protocol classification of states of consciousness. *Brain*. 2018;141(11):3179-3192. doi:10.1093/brain/awy251
39. Gramfort A, Luessi M, Larson E, et al. MNE software for processing MEG and EEG data. *NeuroImage*. 2014;86:446-460. doi:10.1016/j.neuroimage.2013.10.027
40. Pedregosa F, Varoquaux G, Gramfort A, et al. Scikit-learn: Machine Learning in Python. *Mach Learn PYTHON*.:6.
41. Deco G, Kringelbach ML. Metastability and Coherence: Extending the Communication through Coherence Hypothesis Using A Whole-Brain Computational Perspective. *Trends Neurosci*. 2016;39(3):125-135. doi:10.1016/j.tins.2016.01.001
42. Bzdok D, Yeo BTT. Inference in the age of big data: Future perspectives on neuroscience. *NeuroImage*. 2017;155:549-564. doi:10.1016/j.neuroimage.2017.04.061
43. Engemann DA, Kozynets O, Sabbagh D, et al. Combining magnetoencephalography with magnetic resonance imaging enhances learning of surrogate-biomarkers. *eLife*. 2020;9:e54055. doi:10.7554/eLife.54055
44. Fischer D, Edlow BL, Giacino JT, Greer DM. Neuroprognostication: a conceptual framework. *Nat Rev Neurol*. Published online March 29, 2022. doi:10.1038/s41582-022-00644-7